

## Valence instability of $\text{YbCu}_2\text{Si}_2$ through its magnetic quantum critical point

A. Fernandez-Pañella,<sup>1</sup> V. Balédent,<sup>2</sup> D. Braithwaite,<sup>1,\*</sup> L. Paolasini,<sup>3</sup> R. Verbeni,<sup>3</sup> G. Lapertot,<sup>1</sup> and J.-P. Rueff<sup>2,4</sup>

<sup>1</sup>*SPSMS, UMR-E CEA/UJF-Grenoble 1, INAC, 38054 Grenoble, France*

<sup>2</sup>*Synchrotron SOLEIL, L'Orme des Merisiers, Saint-Aubin, Boîte Postale 48, 91192 Gif-sur-Yvette Cedex, France*

<sup>3</sup>*ESRF, 6 rue Jules Horowitz, Boîte Postale 220, 38043 Grenoble Cedex, France*

<sup>4</sup>*Laboratoire de Chimie Physique–Matière et Rayonnement, CNRS-UMR 7614, UPMC, 75005 Paris, France*

(Received 6 June 2012; revised manuscript received 1 August 2012; published 6 September 2012)

We provide a complete picture of the valence instabilities of Yb in the heavy-fermion compound  $\text{YbCu}_2\text{Si}_2$  by resonant inelastic x-ray scattering measurements (RIXS) at the Yb  $L_3$  edge under high pressure (up to 22 GPa) and at low temperatures (down to 7 K) in the vicinity of the magnetic ordered state. The valence shows a significant increase with pressure without reaching the full trivalent state even at the highest pressure. Its pressure dependence is marked by a pronounced change of slope around 10 GPa, a value close to the magnetic critical pressure  $P_c \approx 8$  GPa. Our results suggest that magnetic order in  $\text{YbCu}_2\text{Si}_2$  appears for a valence value  $\nu < 3$ . Unlike  $\text{CeCu}_2\text{Si}_2$ , valence fluctuations do not sustain superconductivity, which is likely destroyed by ferromagnetism.

DOI: [10.1103/PhysRevB.86.125104](https://doi.org/10.1103/PhysRevB.86.125104)

PACS number(s): 71.27.+a, 71.28.+d, 78.70.Ck

### I. INTRODUCTION

The 122 rare-earth-based family (with the general formula  $RM_2X_2$ , with  $R = \text{Ce, Yb}$ ,  $M = \text{transition metal}$ , and  $X = \text{Si, Ge}$ ) has attracted much attention as it effectively concentrates most of the salient features of heavy-fermion (HF) complexity, including strong correlations, magnetic fluctuations, unconventional superconductivity, and non-Fermi-liquid behavior. The Doniach diagram is considered as the “standard model” of the general HF behavior. It depicts the competition between Kondo screening and long-range Ruderman-Kittel-Kasuya-Yoshida (RKKY) magnetic interactions depending on a control parameter, identified here with pressure. Upon the parameter change, the system evolves from a magnetically ordered phase (Kondo lattice) to a nonmagnetic, intermediate-valent (IV) state. Most of the emphasis has been put recently on the electronic behavior in the intermediate region, signaled by a magnetic quantum critical point (QCP) at pressure  $P_c$ , where the magnetic order vanishes. This applies to the 122 family, among which  $\text{CeCu}_2\text{Si}_2$  is the most famous member as the first HF superconductor ever discovered.<sup>1</sup> Superconductivity in  $\text{CeCu}_2\text{Si}_2$  arises below 0.65 K, near the magnetic QCP,<sup>1-4</sup> a common finding in many other Ce-based antiferromagnetic (AF) HF systems. In  $\text{CeCu}_2\text{Si}_2$ , however, the superconducting dome extends away from the magnetically ordering phase, leading to a resurgence of the critical superconducting temperature  $T_c$  at high pressure around  $P_v \approx 4.5$  GPa. While the strong magnetic fluctuations are conventionally held responsible for the electron pairing near the magnetic QCP, the nature of the second dome is far more intriguing. In a recent study in  $\text{CeCu}_2\text{Si}_2$ ,<sup>5</sup> we have demonstrated that the second dome is tightly connected to valence fluctuations, in agreement with recent theoretical interpretation.<sup>6,7</sup> A full description of HF behavior around the QCP, however, involves both magnetic and charge instabilities, and their interplay has not been fully resolved so far. In this respect, comparing  $\text{CeCu}_2\text{Si}_2$  with its hole equivalent  $\text{YbCu}_2\text{Si}_2$  is meaningful as it may help to disentangle the effects of magnetic and charge degrees of freedom and improve the understanding of critical phenomena.  $\text{YbCu}_2\text{Si}_2$  is a moderately heavy fermion

( $\gamma \approx 135 \text{ mJ mol}^{-1} \text{K}^{-2}$ ),<sup>8</sup> and as expected from the electron-hole symmetry, the application of pressure shall produce a mirror image of a cerium phase diagram, as confirmed experimentally. Especially, pressure is expected to lead Yb from nonmagnetic  $\text{Yb}^{2+}(4f^{14})$  to magnetic  $\text{Yb}^{3+}(4f^{13})$  states, while it shows the opposite tendency in the Ce counterpart, with Ce adopting  $\text{Ce}^{3+}(4f^1)$  configuration at large volumes and  $\text{Ce}^{4+}(4f^0)$  at small volumes. Indeed it was confirmed that  $\text{YbCu}_2\text{Si}_2$  exhibits decreasing Kondo temperature with pressure (see Fig. 1) and increasing magnetic fluctuation contributions to the resistivity, and for pressures above 8 GPa magnetic order arises.<sup>9-11</sup>

However, notable differences exist between both systems, such as the stronger localization of the  $4f$  electrons in Yb and a larger spin-orbit coupling, which lead to a different hierarchy of the significant energy scales, i.e., Kondo temperature and crystal electric field (CEF).<sup>14</sup> Therefore, pressure is expected to induce larger valence changes in Yb-based compounds with respect to Ce-based compounds. Moreover, while superconductivity appears almost to be the rule rather than the exception near the QCP in Ce systems, up to now, only one Yb system exhibits such a behavior.<sup>15</sup> An additional difference is the recent discovery of ferromagnetism in  $\text{YbCu}_2\text{Si}_2$ ,<sup>12</sup> while  $\text{CeCu}_2\text{Si}_2$ , like most cerium systems, shows antiferromagnetic properties. The knowledge of the pressure dependence of the rare-earth (RE) valence is key to quantifying the hybridization between the  $f$  electron and the conduction band<sup>16-18</sup> and thus Kondo related effects. The recent development of truly bulk sensitive and resonant spectroscopic techniques has significantly improved the accuracy of RE valence estimation.<sup>17,19,20</sup>

In this work, we investigate the Yb valence changes in  $\text{YbCu}_2\text{Si}_2$  throughout the phase diagram, from deep inside the paramagnetic state to well above the critical pressure and, importantly, at low temperatures, almost down to the ordering temperature (see red points in Fig. 1), using resonant inelastic x-ray scattering (RIXS). The results demonstrate the strong interplay between magnetism and valence properties in  $\text{YbCu}_2\text{Si}_2$ . In Fig. 1 we sketch the  $(P, T)$  phase diagram of  $\text{YbCu}_2\text{Si}_2$ , showing the important temperatures and pressures.

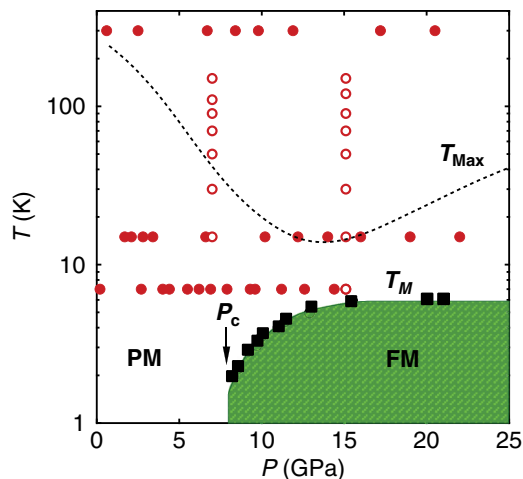


FIG. 1. (Color online)  $P$ - $T$  phase diagram of  $\text{YbCu}_2\text{Si}_2$  (adapted from Ref. 12 for  $P < 13$  GPa and from Ref. 13 for  $P > 13$  GPa).  $T_M$  (squares) and  $P_c$  are the ferromagnetic order temperature and the critical pressure, respectively. Solid circles indicate the  $(P, T)$  loci where the valence was measured at constant temperature (300, 15, and 7 K), and open circles are the temperature dependence at constant pressure (7 and 15 GPa).  $T_{\text{Max}}$  (Ref. 9) is related to the Kondo temperature. See details in text.

The ordering temperature for  $P < 13$  GPa has been measured on single crystals of the same batch as those studied here.<sup>12</sup> As discussed in Ref. 12, the magnetic ordering temperature is higher than that reported in most previous studies but is compatible with the results of Winkelman *et al.*,<sup>13</sup> whose data we have taken for the high-pressure part of the diagram.

## II. EXPERIMENTAL DETAILS

As the energy scales and the magnetic ordering temperature are low, it is important to combine both conditions of high pressure and low temperature. Early measurements in  $\text{YbCu}_2\text{Si}_2$  (Refs. 17 and 21) and in the sibling compounds  $\text{YbNi}_2\text{Ge}_2$  and  $\text{YbPd}_2\text{Si}_2$  (Ref. 22) at ambient pressure already pointed out a continuous valence decrease with temperature, while under pressure, Yb is shown to approach a trivalent configuration in both  $\text{YbNi}_2\text{Ge}_2$  and  $\text{YbPd}_2\text{Si}_2$  (at 300 K). But all these measurements were taken far from the critical region, in either pressure or temperature parameter space, to provide an accurate description of the low-energy interactions and of their interplay. In contrast here, the data were obtained at high-pressure and low-temperature conditions, very close to the ferromagnetic order state, as indicated in the phase diagram in Fig. 1. We have used high-quality single crystals grown by an In-flux method (using MgO crucibles) as described in detail elsewhere.<sup>11</sup> No signs of residual indium were detected either as parasitic phases by x-ray characterization or as a spurious superconducting transition in the resistivity. Moreover, the extremely high value of the residual resistivity ratio ( $>200$ ) indicates a very high crystal purity, implying no (or only extremely limited) indium substitution on the Si or Cu sites. The spectroscopic measurements were performed at the ID16 beam line of the European Synchrotron Radiation Facility (ESRF, Grenoble, France). The undulator beam was monochromatized with a pair of Si(111) crystals and focused to a size of  $40 \mu\text{m}$

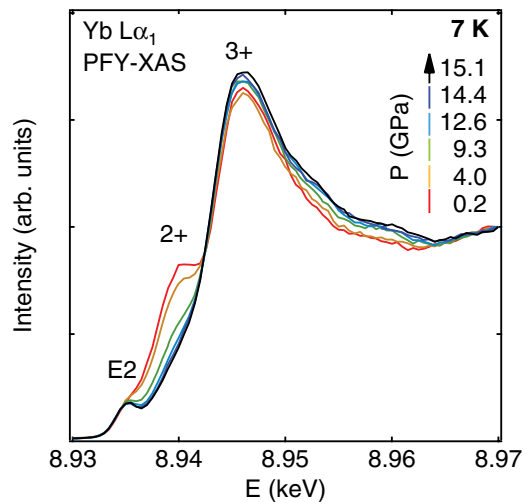


FIG. 2. (Color online) PFY-XAS spectra measured at 7 K at selected pressures. The center position of  $\text{Yb}^{2+}$  and  $\text{Yb}^{3+}$  components are indicated along with the assumed quadrupolar peak E2.

(vertical) and  $100 \mu\text{m}$  (horizontal) at the sample position. The scattered x-rays were analyzed by a Rowland circle spectrometer equipped with a spherically bent Si (620) crystal. The energy resolution was about 1.5 eV. A sample  $\sim 20 \mu\text{m}$  thick was loaded in a membrane-driven diamond-anvil cell (DAC) with silicon oil as a pressure-transmitting medium. The DAC was mounted in a helium circulation cryostat for low-temperature measurements. The lowest temperature achieved was 7 K. Pressure was estimated from the fluorescence of a ruby chip placed in the pressure chamber.

## III. RESULTS AND DISCUSSION

The first sign of the mixed valent state can be observed in the absorption spectra at the Yb  $L_3$  edge. The spectra were recorded in the partial fluorescence (PFY) mode at the Yb  $L\alpha_1$  line in order to reduce lifetime broadening effects and sharpen the spectroscopic features.<sup>19</sup> As shown in Fig. 2, the spectral line shape presents a double-edge structure reminiscent of an admixture of  $\text{Yb}^{2+}$  and  $\text{Yb}^{3+}$  ions. A weak feature on the low-energy side of the  $\text{Yb}^{2+}$  peak denoted E2 in Fig. 2 is related to quadrupolar transition towards empty  $\text{Yb}^{3+}$ ,  $4f$  states. We notice a strong variation of the  $\text{Yb}^{2+}$  to  $\text{Yb}^{3+}$  intensity ratio with increasing pressure, signaling the progressive conversion towards the  $\text{Yb}^{3+}$  state. Although the valence can, in principle, be extracted from the PFY x-ray absorption spectroscopy (XAS) spectra, the method is somewhat complicated by the uncertainty about the position of the edge step. A better way is to utilize the resonant emission spectra instead. The main advantage of the resonant regime (RIXS) is the possibility to selectively enhance either the  $\text{Yb}^{2+}$  ( $2p^6 f^{14} 5d^0$ ) or the  $\text{Yb}^{3+}$  ( $2p^6 f^{13} 5d^1$ ) component by an appropriate choice of the incident photon energy  $h\nu_{\text{in}}$ , thus providing a high accuracy in the estimation of the valence. The Yb  $L\alpha_1$  RIXS spectra measured at the  $\text{Yb}^{2+}$  resonance ( $h\nu_{\text{in}} = 8.9404$  keV) are summarized in Fig. 3 for different pressure and temperature conditions. The two main features peaking at an energy transfer,  $E_t = h\nu_{\text{in}} - h\nu_{\text{out}}$ , of 1525.5 and 1530.5 eV correspond to transitions from the  $\text{Yb}^{2+}$  and  $\text{Yb}^{3+}$  components

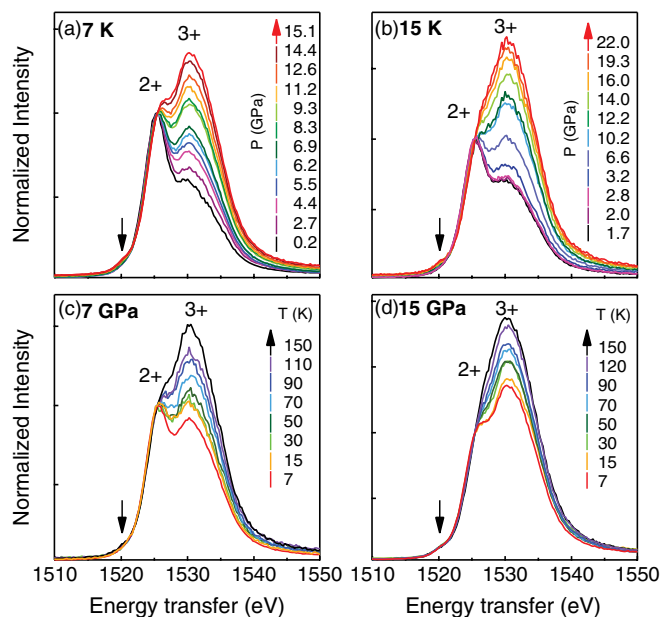


FIG. 3. (Color online) Pressure and temperature dependence of the Yb  $L\alpha_1$  RIXS spectra in  $\text{YbCu}_2\text{Si}_2$ . The four panels summarize the results obtained at a constant temperature of (a) 7 K and (b) 15 K and a constant pressure of (c) 7 GPa and (d) 15 GPa. The arrow indicates the quadrupolar peak  $E_2$ .

of the initial mixed valent ground state  $|g\rangle = a|f^{13}\rangle + b|f^{14}\rangle$ . To enhance spectral changes in Fig. 3, all the spectra are normalized to the  $\text{Yb}^{2+}$  intensity and plotted versus  $E_t$ . The vertical arrow around  $E_t = 1520$  eV indicates the position of the quadrupole-allowed transition ( $E_2$ )  $2p^6 4f^{13} \rightarrow 2p^5 4f^{14}$  of  $\text{Yb}^{3+}$ . In the resonant regime this feature is much weaker than in the PFY spectra. We observe a clear increase of the  $\text{Yb}^{3+}$  intensity under pressure with respect to  $\text{Yb}^{2+}$  at all measured temperatures [7, 15, and 300 K (not shown)], while the weak  $E_2$  feature stays mostly unchanged. This transfer of spectral weight is consistent with the expected delocalization of  $4f$  electrons under pressure and increase of Yb valence. In contrast, the Yb valence is found to decrease upon cooling at 7 and 15 GPa, following the reported trend at ambient pressure<sup>17</sup> towards a divalent state. We now turn to the quantitative investigation of Yb valence as a function of both pressure and temperature. The valence was extracted from the RIXS data using the expression  $v = 2 + I^{3+}/(I^{2+} + I^{3+})$ , where  $I^{2+}$  and  $I^{3+}$  are the integrated intensities of the pure-valent spectral components. These were evaluated by fitting the data with two Gaussian line shapes centered on the 2+ and 3+ peaks; the background contribution was taken into account by an arctangent function. The  $E_2$  feature was disregarded in the analysis because of its negligible contribution. The results, summarized in Fig. 4, provide a comprehensive picture of  $f$ -electron delocalization near the critical region at high pressure and low temperature. First, they show a monotonous increase of the valence under pressure towards trivalency, independent of temperature, as we previously inferred from the spectra inspection. At all temperatures, the  $v(P)$  dependence shows a strong and close-to-linear increase at low pressures, followed by a much weaker increase at high pressures. This change of slope occurs in a relatively small pressure window

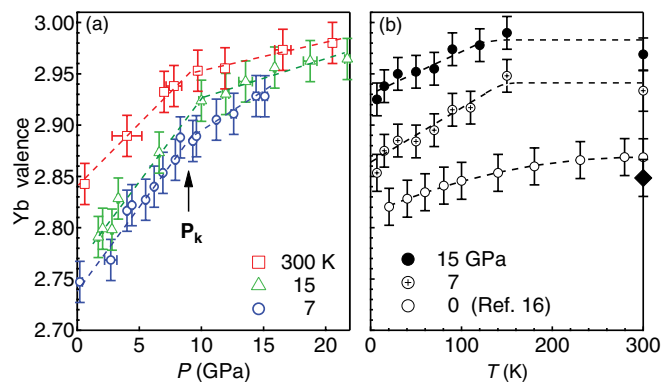


FIG. 4. (Color online) (a) Valence-pressure dependence of  $\text{YbCu}_2\text{Si}_2$  at 7, 15, and 300 K. The arrow indicates the pressure where a kink is observed ( $P_k$ ). (b) Valence-temperature dependence at 15 and 7 GPa and at ambient pressure (open circles;<sup>17</sup> the black diamond is the value we obtained in this work). Dashed lines are guides to the eyes.

(9–11 GPa) for all the temperatures we measured. It is particularly visible at 15 K, where the kink (defined as  $P_k$  in the following) is found at  $\sim 10$  GPa, a pressure comparable to  $P_c$ . Above  $P_k$  the valence keeps increasing, but more slowly, reaching 2.95 even at the highest measured pressure, 22 GPa, in the vicinity of the magnetic ordered phase. Thus, in the high-pressure region of the phase diagram, magnetism is found to set in for a noninteger valence  $v < 3$ .<sup>23</sup> As discussed in detail by Flouquet and Harima,<sup>14</sup> this may be the main difference compared to cerium systems, as the hierarchy of the energy scales in Yb may allow the formation of the heavy fermion and the magnetically ordered state for a much wider range of the Yb valence than in Ce. This is a strong motivation for further studies to compare the macroscopic phase diagrams with the valence state measured at high pressure and low temperature in other ytterbium systems where magnetic order is induced with pressure, such as  $\text{YbInCu}_4$ , where the valence transition at ambient pressure is already well documented.<sup>17</sup>

In Fig. 4(b), the temperature dependence of the valence at constant pressure further highlights the interplay of the significant energy scales. At all pressures the valence decreases with decreasing temperature. The previous measurement at ambient pressure<sup>17</sup> found that this decrease occurs mainly in the temperature range  $T < 150$  K. In the present study we focus more specifically on the low-temperature side below 150 K. We do, however, find at all pressures a decrease of the valence in the temperature range 7–150 K, at least as strong as that found at ambient pressure, and virtually no temperature change of the valence between 150 and 300 K. This implies that the temperature where the valence starts to decrease is relatively insensitive to pressure and so is probably not directly related to the Kondo temperature, which strongly decreases with pressure (see Fig. 1). These features are likely related to CEF effects and to the localized behavior of the  $4f$  electrons at high temperature, leading to the system favoring an integer valence. In fact, neutron measurements<sup>24,25</sup> have revealed that the first excited doublet in  $\text{YbCu}_2\text{Si}_2$  is located around 140 K, and the second one is above 300 K. Thus, the initial increase of  $|\partial v/\partial T|$  between 0 and 7 GPa is understood as being due to increasing magnetic fluctuations.

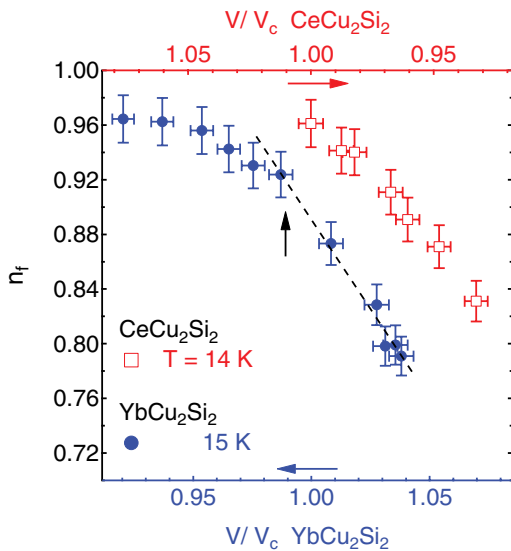


FIG. 5. (Color online) The  $f$  electron and hole occupancy of  $\text{CeCu}_2\text{Si}_2$  (top axis) and  $\text{YbCu}_2\text{Si}_2$  (bottom axis) vs their molar volume normalized to their critical molar volume  $V_c$  (see details in text) at  $T \approx 15$  K. The blue and red arrows indicate the direction of increasing applied external pressure for  $\text{YbCu}_2\text{Si}_2$  and  $\text{CeCu}_2\text{Si}_2$ , respectively, while the vertical black arrow indicates the volume which corresponds to  $P_k \approx 10$  GPa (from Fig. 3). The dashed black line is a linear fit for  $V > V_c$ . See details in the text.

Recent valence measurements carried out in  $\text{CeCu}_2\text{Si}_2$  in similar extreme conditions<sup>5</sup> offer the valuable opportunity to draw a direct comparison between  $4f$  electron (Ce) and hole (Yb) occupancy,  $n_f$ . As  $\text{YbCu}_2\text{Si}_2$  (bulk modulus  $B_0 = 168$  GPa)<sup>10</sup> is harder than  $\text{CeCu}_2\text{Si}_2$  ( $B_0 = 112$  GPa),<sup>26</sup> it is more appropriate to compare their  $n_f$  in respect to their relative critical volume change rather than the applied external pressure, as shown in Fig. 5.  $V_c$  for  $\text{YbCu}_2\text{Si}_2$  is taken as  $145.97 \text{ \AA}^3$ , the cell volume at 8 GPa, whereas for  $\text{CeCu}_2\text{Si}_2$  we take the volume at ambient pressure ( $165.324 \text{ \AA}^3$ ), assuming the critical pressure is close to  $P_c = 0$ . The upper axis has been shifted in order to align the critical molar volume for both compounds. The blue and red arrows indicate the increasing direction for pressure for  $\text{YbCu}_2\text{Si}_2$  and  $\text{CeCu}_2\text{Si}_2$ , respectively. Our results show that the volume effect on the

valence for both systems is actually quite similar. However, in  $\text{YbCu}_2\text{Si}_2$ , the change of  $n_f$  versus the relative volume change in the region  $V > V_c$  is about 50% larger than in  $\text{CeCu}_2\text{Si}_2$ , and at  $V_c$ , the value of  $n_f$  is much closer to 1 in  $\text{CeCu}_2\text{Si}_2$  (0.96) than in  $\text{YbCu}_2\text{Si}_2$  (0.90). As we have already emphasized in  $\text{YbCu}_2\text{Si}_2$ , magnetic order is likely to appear before the trivalent state is reached. For  $\text{YbCu}_2\text{Si}_2$  the slope change of  $v(P)$  seen in Fig. 4 is also apparent in the  $n_f(V/V_c)$  dependence as the deviation from the linear behavior (dashed black line) at a  $V/V_c \approx 0.99$ , which corresponds to  $P_k$  (indicated by the black arrow in Fig. 5). Further studies in other compounds would be of great interest in order to clarify if this is a general tendency in Ce and Yb systems or a particular trend of the 122 family. The most striking result is the different positions of the critical volume in relation to the valence change. From these results, it is tempting to conclude that valence fluctuations in  $\text{YbCu}_2\text{Si}_2$  could seed unconventional superconductivity at high pressure, as theoretically predicted in the 122 family<sup>6,7</sup> and experimentally confirmed in  $\text{CeCu}_2\text{Si}_2$ .<sup>5</sup> Yet the lack of any evidence of superconductivity in  $\text{YbCu}_2\text{Si}_2$  so far<sup>11</sup> shows that valence fluctuations do not suffice, and other phenomena, notably the predominance of ferromagnetic correlations, may in fact prevent superconductivity. In conclusion, this work provides the most complete picture so far of valence instability near the critical region and the magnetic order phase of a heavy-fermion system,  $\text{YbCu}_2\text{Si}_2$ . A significant valence change under pressure of the  $f$ -electron occupancy is observed, with a distinctive change of slope close to the critical pressure where magnetic order occurs. The fully trivalent state is not yet achieved at the highest pressure of this study, showing that  $\text{YbCu}_2\text{Si}_2$  remains in a weak Kondo regime for a wide range of its phase diagram, also in the magnetic ordered phase. Unlike  $\text{CeCu}_2\text{Si}_2$ , valence fluctuations do not sustain superconductivity in  $\text{YbCu}_2\text{Si}_2$ .

## ACKNOWLEDGMENTS

We thank J. Flouquet, H. Harima, and S. Burdin for fruitful discussions. This work was supported by the French ANR agency within the project Blanc PRINCESS.

\*Corresponding author: daniel.braithwaite@cea.fr

<sup>1</sup>F. Steglich, J. Aarts, C. D. Bredl, W. Lieke, D. Meschede, W. Franz, and H. Schäfer, *Phys. Rev. Lett.* **43**, 1892 (1979).

<sup>2</sup>B. Bellarbi, A. Benoit, D. Jaccard, J. M. Mignot, and H. F. Braun, *Phys. Rev. B* **30**, 1182 (1984).

<sup>3</sup>H. Q. Yuan, F. M. Grosche, M. Deppe, C. Geibel, G. Sparn, and F. Steglich, *Science* **302**, 2104 (2003).

<sup>4</sup>K. Fujiwara, Y. Hata, K. Kobayashi, K. Miyoshi, J. Takeuchi, Y. Shimaoka, H. Kotegawa, T. C. Kobayashi, C. Geibel, and F. Steglich, *J. Phys. Soc. Jpn.* **77**, 123711 (2008).

<sup>5</sup>J.-P. Rueff, S. Raymond, M. Taguchi, M. Sikora, J.-P. Itié, F. Baudelet, D. Braithwaite, G. Knebel, and D. Jaccard, *Phys. Rev. Lett.* **106**, 186405 (2011).

<sup>6</sup>T. A. Holmes, D. Jaccard, and K. Miyake, *J. Phys. Soc. Jpn.* **76**, 051002 (2007).

<sup>7</sup>S. Watanabe and K. Miyake, *J. Phys. Condens. Matter* **23**, 094217 (2011).

<sup>8</sup>B. Sales and R. Viswanathan, *J. Low Temp. Phys.* **23**, 449 (1976).

<sup>9</sup>K. Alami Yadri, H. Wilhelm, and D. Jaccard, *Eur. Phys. J. B* **6**, 5 (1998).

<sup>10</sup>J. Sanchez and M. Abd-Elmeguid, *Hyperfine Interact.* **128**, 137 (2000).

<sup>11</sup>E. Colombier, D. Braithwaite, G. Lapertot, B. Salce, and G. Knebel, *Phys. Rev. B* **79**, 245113 (2009).

<sup>12</sup>A. Fernandez-Pañella, D. Braithwaite, B. Salce, G. Lapertot, and J. Flouquet, *Phys. Rev. B* **84**, 134416 (2011).



- <sup>13</sup>H. Winkelmann, M. M. Abd-Elmeguid, H. Micklitz, J. P. Sanchez, P. Vulliet, K. Alami-Yadri, and D. Jaccard, *Phys. Rev. B* **60**, 3324 (1999).
- <sup>14</sup>J. Flouquet and H. Harima, arXiv:0910.3110.
- <sup>15</sup>S. Nakatsuji, K. Kuga, Y. Machida, T. Tayama, T. Sakakibara, Y. Karaki, H. Ishimoto, S. Yonezawa, Y. Maeno, E. Pearson, G. Lonzarich, L. Balicas, H. Lee, and Z. Fisk, *Nat. Phys.* **4**, 603 (2008).
- <sup>16</sup>C. Dallera, M. Grioni, A. Shukla, G. Vankó, J. L. Sarrao, J. P. Rueff, and D. L. Cox, *Phys. Rev. Lett.* **88**, 196403 (2002).
- <sup>17</sup>L. Moreschini, C. Dallera, J. J. Joyce, J. L. Sarrao, E. D. Bauer, V. Fritsch, S. Bobev, E. Carpena, S. Huotari, G. Vankó, G. Monaco, P. Lacovig, G. Panaccione, A. Fondacaro, G. Paolicelli, P. Torelli, and M. Grioni, *Phys. Rev. B* **75**, 035113 (2007).
- <sup>18</sup>K. Kummer, Y. Kucherenko, S. Danzenbächer, C. Krellner, C. Geibel, M. G. Holder, L. V. Bekenov, T. Muro, Y. Kato, T. Kinoshita, S. Huotari, L. Simonelli, S. L. Molodtsov, C. Laubschat, and D. V. Vyalikh, *Phys. Rev. B* **84**, 245114 (2011).
- <sup>19</sup>J.-P. Rueff and A. Shukla, *Rev. Mod. Phys.* **82**, 847 (2010).
- <sup>20</sup>J.-P. Rueff, J.-P. Itié, M. Taguchi, C. F. Hague, J.-M. Mariot, R. Delaunay, J.-P. Kappler, and N. Jaouen, *Phys. Rev. Lett.* **96**, 237403 (2006).
- <sup>21</sup>J. M. Lawrence, G. H. Kwei, P. C. Canfield, J. G. DeWitt, and A. C. Lawson, *Phys. Rev. B* **49**, 1627 (1994).
- <sup>22</sup>H. Yamaoka, I. Jarrige, N. Tsujii, J.-F. Lin, N. Hiraoka, H. Ishii, and K.-D. Tsuei, *Phys. Rev. B* **82**, 035111 (2010).
- <sup>23</sup>As these measurements were performed at a temperature slightly above  $T_M$ , we cannot exclude that the valence will further increase or even jump to 3 at the onset of the magnetic order, although this seems unlikely. A valence less than 3 could also arise from phase mixture. A Mössbauer study (Ref. 10) found a magnetic component and a nonmagnetic component just above  $P_c$ . However, this would imply that this phase separation exists even at 22 GPa, which also seems extremely unlikely.
- <sup>24</sup>E. Holland-Moritz, D. Wohlleben, and M. Loewenhaupt, *Phys. Rev. B* **25**, 7482 (1982).
- <sup>25</sup>A. Muzychka, *J. Exp. Theor. Phys.* **87**, 162 (1998).
- <sup>26</sup>S. Tsuduki, A. Onodera, K. Ishida, Y. Kitaoka, A. Onuki, N. Ishimatsu, and O. Shimomura, *Solid State Commun.* **134**, 747 (2005).